DNA Polymerase β: Pre-Steady-State Kinetic Analyses of dATPαS Stereoselectivity and Alteration of the Stereoselectivity by Various Metal Ions and by Site-Directed Mutagenesis†

Jia Liu‡ and Ming-Daw Tsai*

Departments of Biochemistry and Chemistry, Ohio State Biochemistry Program, and Protein Research Group, The Ohio State University, Columbus, Ohio 43210

Received March 30, 2001; Revised Manuscript Received June 5, 2001

ABSTRACT: The first pre-steady-state kinetic analysis of the stereoselectivity of a DNA polymerase, Pol β from rat brain, toward Rp and Sp isomers of dATPαS, and alteration of the stereoselectivity by various metal ions and by site-directed mutagenesis are reported. Diastereomers of dATPαS were synthesized by enzymatic methods to >98% purity. The rate of polymerization (k_{pol}) and the apparent dissociation constant ($K_{d,app}$) were measured with dATP, Rp-dATPαS, and Sp-dATPαS in the presence of Mg^{2+}, Mn^{2+}, or Cd^{2+}. The results indicate that wild type (WT) polymerase (Pol) β can incorporate both Sp- and Rp-dATPαS in the presence of Mg^{2+}, but Sp is the preferred isomer. The stereoselectivity, defined as $(k_{pol}/K_d)_{Sp}/(k_{pol}/K_d)_{Rp}$ (abbreviated Sp/Rp ratio), is 57.5 in the presence of Mg^{2+}. When Mg^{2+} was substituted with Mn^{2+} and Cd^{2+}, the Sp/Rp ratio decreased to 7.6 and 21, respectively. These results are discussed in relation to the crystal structures of various Pol β complexes, as well as previous steady-state kinetic studies of other DNA polymerases. In addition, the D276R mutant was designed to introduce a potential extra hydrogen bonding interaction between the arginine side chain and the pro-Sp oxygen of the α-phosphate of dNTP. The kinetic data of the D276R mutant showed a pronounced relaxation of stereoselectivity of dATPαS (Sp/Rp ratio = 1.5, 3.7, and 1.5 for Mg^{2+}, Mn^{2+}, and Cd^{2+}, respectively). Furthermore, the D276R mutant showed a 5-fold enhanced reactivity toward Rp-dATPαS relative to WT Pol β, suggesting that this mutant Pol β can be used to incorporate Rp-dNTPαS into DNA oligomers.

DNA polymerase β (Pol β)[1] catalyzes the template-directed nucleotidyl transfer reaction and performs an essential part of the DNA repair process in filling single-stranded gaps in the base excision repair process (*2*−*4*). Extensive kinetic studies and in vivo mutation assays of the wild-type protein and different mutants have been performed to elucidate the catalytic mechanism and fidelity of Pol β (*5*−*10*). Several crystal structures, including binary and ternary complexes of Pol β, have been solved in the past several years (*11*−*13*). Like most other polymerases, Pol β consists of three distinct subdomains (designated thumb, palm, and fingers), forming a DNA binding channel. It should be noted that in our earlier publications we have followed the designation of thumb and fingers subdomains of Pelletier et al. (*11*), whereas in the present paper we switch to that of Steitz et al. (*14*) to facilitate a more accurate comparison between Pol β and other polymerases.

The requirement of divalent metal ions for catalysis was first recognized in the early study of *Escherichia coli* DNA polymerase I (Pol I) (*15*). Subsequent studies with other polymerases confirmed that Mg^{2+} is likely the divalent metal ion utilized by most polymerases for catalysis in vivo (*16*). On the basis of the structures of ternary complexes of Pol β with DNA and ddCTP substrates (*13*), specific roles have been assigned for two Mg^{2+} ions in the active site of Pol β as shown in Figure 1. Recently we have shown that binding of Cr(III)dNTP alone (before binding of the second metal ion) to Pol β is sufficient to induce the closing of the fingers subdomain (*1*).

Stereoselectivity of an enzyme toward Rp and Sp isomers of phosphorothioate analogues of dNTP, coupled with variation of metal ions, has long been established as a useful tool in probing detailed interactions between metal ions and nucleotides at the active site of enzymes (*17*−*21*). However, this approach has not been used for DNA polymerases, except for early steady-state kinetic studies of *E. coli* Pol I (*22*) and phage T4 DNA polymerase (*23*). The results of these studies indicated that DNA polymerases accept the Sp isomer of dNTPαS exclusively, even when Mg^{2+} was replaced by Co^{2+} or Mn^{2+}, which has a higher preference for sulfur ligands. As pointed out by Pelletier et al. (*24*), this result appeared to be in contradiction with the observa-

† This work was supported by NIH Grant GM43268. This is paper 9 in the series "DNA Polymerase β". For paper 8, see Arndt et al. (*1*).

* Author to whom correspondence should be addressed at the Department of Chemistry [telephone: (614) 292-3080; fax (614) 292-1532; e-mail tsai.7@osu.edu].

‡ Department of Biochemistry.

[1] Abbreviations: BSA, bovine serum albumin; dAMP, 2′-deoxyadenosine 5′-*O*-phosphate; dAMPS, 2′-deoxyadenosine 5′-*O*-phosphorothioate; dATPαS, 2′-deoxyadenosine 5′-*O*-(1-thiotriphosphate); dNTP, 2′-deoxynucleoside 5′-triphosphate; DTT, dithiothreitol; EDTA, ethylenediaminetetraacetic acid; Hepes, *N*-[2-hydroxyethyl]piperazine-*N*′-[2-ethanesulfonic acid]; Pol I, *Escherichia coli* DNA polymerase I; Pol β, rat DNA polymerase β; RT, reverse transcriptase; S-oligos, phosphorothioate analogues of oligonucleotides; TLC, thin-layer chromatography; Tris, tris(hydroxymethyl)aminomethane; WT, wild type.

10.1021/bi010646j CCC: $20.00
Published on Web 07/04/2001

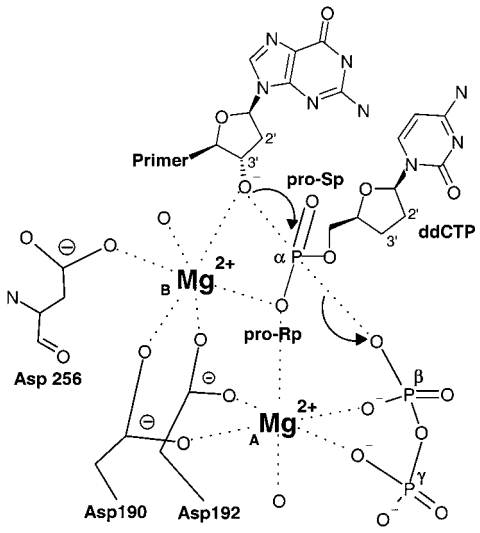

FIGURE 1: Active site of Pol β showing the interactions of the incoming nucleotide with the three aspartic acid residues and the two metal ions (*13*).

tion that when dATPαS was cocrystallized with Pol β in the presence of Mn^{2+}, the Rp isomer instead of the Sp isomer binds to the active site. In this paper we report detailed analyses of the activities of Pol β toward Rp and Sp isomers of dATPαS using pre-steady-state kinetics, seeking to elucidate the stereoselectivity and to understand the metal ion binding properties of Pol β.

The second goal of this paper is to construct mutants of Pol β that will show improved activity toward the disfavored Rp isomer of dATPαS. If a Pol β mutant with improved Rp isomer activity can be obtained, it could potentially lead to the synthesis of "phosphorothioate analogues of oligonucleotides" (abbreviated "S-oligos") from the Rp isomer of dNTPαS. The potential significance of this goal is addressed under Discussion. As an effort toward this goal, the D276R mutant was designed to introduce an extra interaction between the arginine side chain of the enzyme and the α-phosphate of dNTP. Such an interaction, if actually occurring, could perturb the preference of the enzyme toward isomers of dNTPαS. The results indicate that the D276R mutant showed a pronounced relaxation of stereoselectivity of dATPαS and a 5-fold enhanced reactivity toward the Rp isomer relative to WT Pol β.

MATERIALS AND METHODS

Materials. Ultrapure dNTP, dAMPS, dATPαS mixed isomers, nuclease, and protease activity free BSA and G-25 microspin columns were obtained from Pharmacia Biotech. Thermostable *Pfu* DNA polymerase was from Stratagene. [γ-^{32}P]ATP was from ICN Biomedicals. T4 polynucleotide kinase, pyruvate kinase, adenylate kinase, and *Dpn*I exonuclease were purchased from New England Biolabs.

Mutagenesis and Enzyme Preparation. By use of appropriate mutagenic oligonucleotides (IDT Inc.) and wild-type Pol β plasmid [pET-17b(Pol β)] (*25*) as a template, Pol β mutant D276R was created by the "QuikChange" method according to the protocol from Stratagene. The resulting mutation was confirmed by sequencing the entire Pol β gene according to the Sanger method using a 373A DNA sequencer (Applied Biosystems). WT Pol β and mutant Pol β were then overexpressed in an *E. coli* system, BL21(DE3)-[plysS, pET-17b(Pol β)] (*25*) and purified as described previously (*8*). The enzymes were estimated to be >90% homogeneous on the basis of SDS-PAGE analysis developed by the silver-staining method. The exact concentrations of the enzyme solutions were determined by using an extinction coefficient of 21200 M^{-1} cm^{-1} at 280 nm (*26*).

Preparation of Pure Stereoisomers. Sp-dATPαS was synthesized from dAMPS by coupled reactions of adenylate kinase and pyruvate kinase. The reaction mixture contained in 40 mL at room temperature 7.5 mM ATP, 5.0 mM dAMPS, 15 mM phosphoenol pyruvate, 50 mM KCl, 15 mM $MgCl_2$, 30 mM Tris-HCl buffer (pH 8.0), 1 mM DTT, 200 units/mL adenylate kinase, and 10 units/mL pyruvate kinase. The pH of the reaction mixture was adjusted to 8.0 with 0.3 M potassium hydroxide before the enzymes were added. The reaction was followed by thin-layer chromatography on silica gel plates containing a fluorescent indicator with a 1.0 M lithium chloride buffer system. Nucleotides were visualized with UV light. The reaction mixture was then applied to a DEAE-Sephadex A-25 column at 4 °C with a linear gradient of 1.0 L of 0.2 M and 1.0 L of 0.75 M triethylammonium bicarbonate buffers (pH 7.5). The fractions that contained dATPαS were pooled and lyophilized to dryness. Finally, the proton-decoupled ^{31}P NMR was used to check the purity of the product.

Rp-dATPαS was obtained from dATPαS mixed isomers by removing the Sp-dATPαS using adenylate kinase (*27*). The incubation mixture (total volume of 6 mL) contained 3 mM dATPαS (mixture of isomers), 6 mM dAMP, 10 mM DTT, and 50 mM Tris-HCl (pH 8.0). About 300 units of adenylate kinase (100 μL, dialyzed against 10 mM Tris-HCl, pH 8.0, for 2 h prior to use) was added to the reaction mixture. The reaction was followed by TLC as described for the Sp isomer preparation. After 2 h of incubation at room temperature, ~50% dATPαS mixed isomers had been consumed and the reaction mixture was chromatographed on a DEAE-Sephadex column with a linear gradient of 500 mL each of 0.1 and 0.6 M triethylammonium bicarbonate.

DNA Substrates. DNA oligomers were purchased from IDT Inc. (Coralville, IA). Template/primer DNA substrates (annealed heteropolymeric complementary [45mer template]/[25mer primer] duplexes) were used in the experiments. Both oligonucleotides were purified by electrophoresis through denaturing (7 M urea) polyacrylamide gels; a 16% gel was used to purify the 25mer and a 10% gel for the 45mer. Sequences of the substrates used can be found in Werneburg et al. (*25*), and the substrates were prepared as described (*25*).

The 25mer primer was 5′-radiolabeled with [γ-^{32}P]ATP (4500 Ci/mmol) and T4 polynucleotide kinase as described in the manufacturer's protocol. The unreacted [γ-^{32}P]ATP was removed from the 5′-radiolabeled DNA solution with a G-25 microspin column (Pharmacia). The labeled primer DNA was mixed with ~100-fold molar excess of unlabeled DNA (primer and template DNA), and the T4 polynucleotide kinase was inactivated at 80 °C for 5 min. The solution was slowly cooled to room temperature for 2 h to anneal the DNA substrate.

Kinetic Experiments and Product Analysis. A rapid quench instrument (KinTek Instrument Corp., State College, PA) was used for rapid quench experiments with reaction times

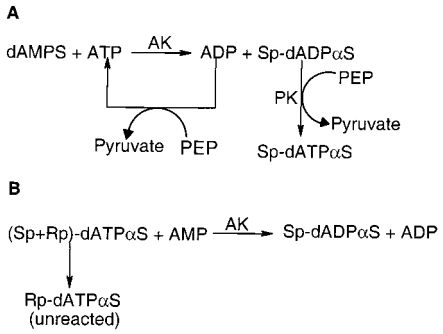

FIGURE 2: Preparation of pure Sp- and Rp-dATPαS diastereomers by enzymatic methods: (A) preparation of Sp isomer from AMPS by the coupled reactions of adenylate kinase (AK) and pyruvate kinase (PK) (PEP, phosphoenol pyruvate); (B) preparation of the Rp isomer by AK-catalyzed consumption of the Sp isomer from the mixture.

ranging from 10 ms to 20 s. The typical experiment was performed at 37 °C in 50 mM Tris-HCl (pH 8.0) containing 50 mM KCl, 10% glycerol, 5.0 mM $MgCl_2$, and various [dNTP]. All concentrations given refer to the final concentrations after mixing. Pol β was preincubated with the DNA substrate prior to rapid mixing with dNTP and divalent metal ions to begin the reaction that was quenched with 0.5 M EDTA. For reaction times >20 s, 20 μL aliquots of the reaction mixture (normally total volume of 300 μL) were removed manually and the reactions were stopped by the addition of 0.5 M EDTA (pH 8.0) after the selected time intervals. The quenched samples were mixed with an equal volume of gel loading buffer and denatured at 85 °C for 5 min, and the products were separated on a 16% polyacrylamide−7 M urea gel. The disappearance of substrate (25mer) and the formation of product (26mer) were analyzed with a STORM 840 PhosphorImager (Molecular Dynamics) to quantify product formation. A ~10-fold excess of the enzyme (1 μM in the reaction mixture) relative to the DNA substrate (100 nM) was used for all assays. Under these conditions, >90% of the DNA substrate should be complexed to the enzyme (*25*), and the reaction time course is represented by a characteristic burst phase of dNTP incorporation only. Thus, the rate of single catalytic turnover is measured.

Data Analysis. Data obtained from kinetic assays were fitted by nonlinear regression using Sigma Plot software (Jandel Scientific) with the appropriate equations. The apparent burst rate constant (k_{obs}) for each particular concentration of dNTP was determined by fitting the time courses for the formation of product (26mer) with eq 1

$$[26\text{mer}] = A[1 - \exp(-k_{obs}t)] \quad (1)$$

where A represents the burst amplitude. The turnover number k_{pol} and apparent dissociation constant for dNTP ($K_{d,app}$) were then obtained from plotting the apparent catalytic rates, k_{obs}, against dNTP concentrations and fitting the data with the hyperbolic eq 2

$$k_{obs} = (k_{pol}[\text{dNTP}])/([\text{dNTP}] + K_{d,app}) \quad (2)$$

RESULTS

Preparation of Diastereomeric Phosphorothioate Analogues. We used enzymatic methods to synthesize pure dATPαS isomers to very high purity, as illustrated in Figure 2. Sp-dATPαS was synthesized from dAMPS by the coupled reactions of adenylate kinase and pyruvate kinase in a procedure modified from that of Brody and Frey (*28*). Rp-dATPαS was purified from commercially available mixed isomers by removing the Sp-dATPαS using adenylate kinase (*27*). The proton-decoupled ^{31}P NMR spectra of purified Sp and Rp isomers are shown in Figure 3 (only P_α regions are shown). No detectable peak from the other isomer was present in either spectrum, and the purity was estimated to be >98% for both isomers on the basis of the signal-to-noise ratio.

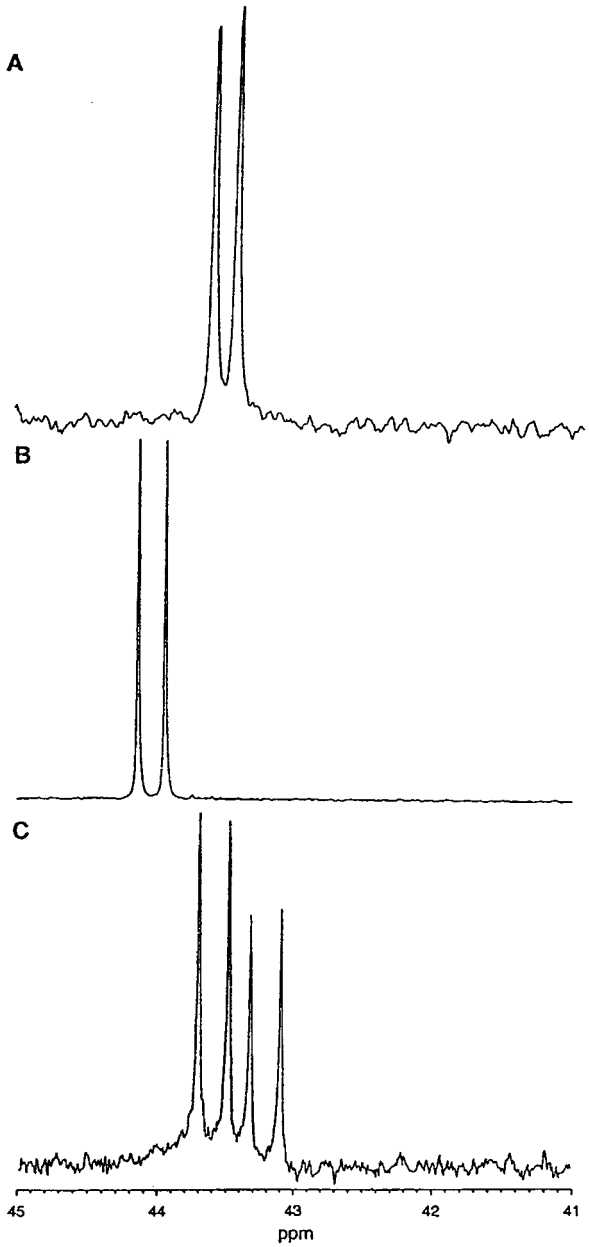

FIGURE 3: ^{31}P NMR spectrum for dATPαS (10 mM Tris, 1 mM EDTA buffer, pH 7.5): (A) purified Rp isomer; (B) purified Sp isomer; (C) mixed isomers. Only the α-phosphate region of the spectrum is shown.

Pre-Steady-State Kinetic Analyses of WT Pol β in the Presence of Different Metal Ions. Pre-steady-state kinetic experiments were first performed to determine the ability of different metal ions to replace Mg^{2+}, as well as the optimal concentration of each metal ion. As shown in Figure 4, Mn^{2+}

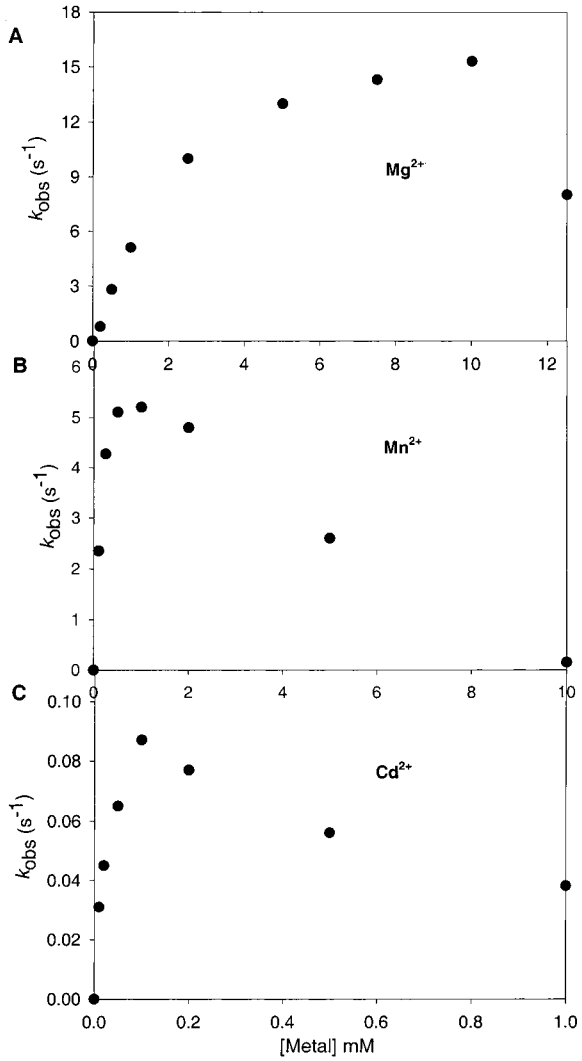

FIGURE 4: Dependence of Pol β activities on Mg^{2+} (A), Mn^{2+} (B), or Cd^{2+} (C). The WT Pol β preincubated with DNA substrate was mixed with metal ion and dATP (200 μM) solutions, and the reaction was quenched after an allotted time. The results were fitted to a single-exponential equation (eq 1) to obtain k_{obs} for each metal ion concentration. The observed catalytic rate (k_{obs}) was then plotted against metal ion concentration. Tris buffer (pH 8.0, 50 mM) was used for Mg^{2+} and Mn^{2+}, whereas Hepes buffer (pH 8.0, 50 mM) was used for Cd^{2+}.

can activate Pol β as well as Mg^{2+} does at low concentrations (<1 mM), in agreement with the observations reported previously (*25*). However, Mn^{2+} becomes inhibitory at concentrations >2 mM, whereas Mg^{2+} reaches its optimal concentration at 9 mM. Pol β activity with Cd^{2+} (0.1−1 mM) in the typical Tris buffer used for other metal ions was extremely low, and almost no turnover was detected during the reaction time (up to 30 min). However, in 50 mM Hepes buffer (pH 8.0) complete turnover of the DNA substrates was observed under single-turnover condition, although with a much lower activity (~100 fold slower than that with Mg^{2+}) and very low optimal concentration (0.1 mM). We then chose the metal ion concentrations that gave optimal activity (1 mM Mn^{2+} and 0.1 mM Cd^{2+}) or close to optimal activity (5 mM Mg^{2+}, 85% optimal activity) for the following studies with different metal ions as well as dNTPαS isomers of WT and mutant Pol β.

The rate of polymerization (k_{pol}) and the apparent dissociation constant of dATP ($K_{d,app}$) were determined by measuring the concentration dependence of dATP incorporation on the rate of the 25/45mer DNA substrate by Pol β under single-turnover conditions. Representative data for the determination of k_{pol} and $K_{d,app}$ are shown in Figure 5. The results of the pre-steady-state kinetic parameters of WT Pol β with dATP in the presence of different metal ions are summarized in Table 1. In the presence of Mn^{2+} Pol β shows k_{pol} and $K_{d,app}$ values very similar to those in the presence of Mg^{2+}, whereas Cd^{2+} shows a much lower activity (400-fold decrease in k_{pol}) but a tighter binding of dATP (20-fold lower $K_{d,app}$).

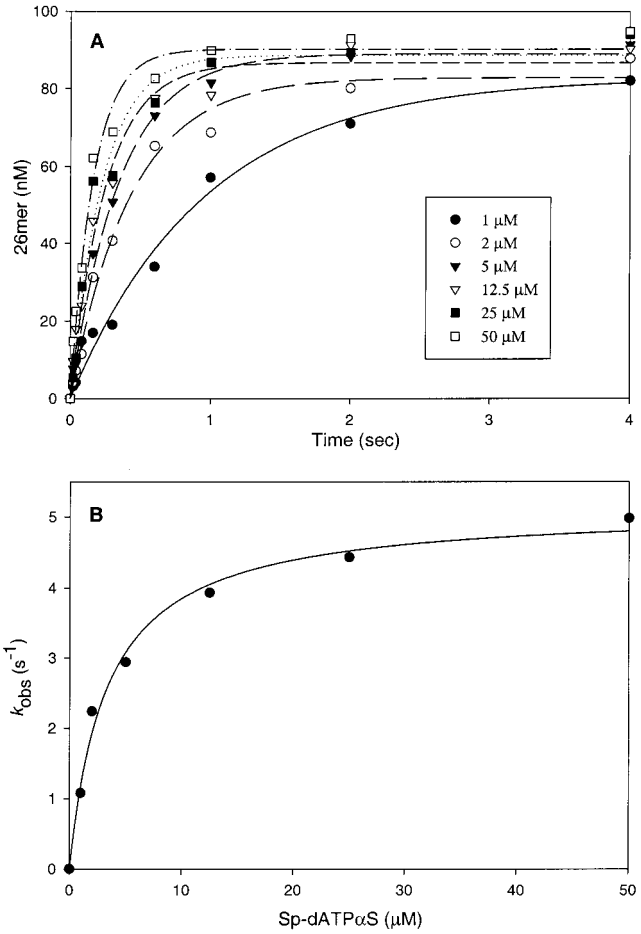

FIGURE 5: Pre-steady-state kinetics of Sp-dATPαS incorporation catalyzed by WT Pol β with Mg^{2+} as the divalent metal ion. The reaction conditions and methods of product analysis were as described under Materials and Methods. (A) Product−time plot. DNA substrate (100 nM) was incubated with 1000 nM Pol β and reacted with 1, 2, 5, 12.5, 25, and 50 μM Sp-dATPαS diastereomeric isomer. The reaction was quenched with 0.5 M EDTA after 0.02, 0.04, 0.08, 0.16, 0.3, 0.6, 1, 2, and 4 s. The results were fitted to a single-exponential equation (eq 1) to obtain k_{obs} for each Sp-dATPαS concentration. (B) Sp-dATPαS concentration dependence curve. k_{pol} and $K_{d,app}$ values were determined as 5.3 ± 0.2 s^{-1} and 3.3 ± 0.4 μM, respectively, by fitting to the hyperbolic equation (eq 2).

Stereoselectivity of WT Pol β toward Stereoisomers of dATPαS in the Presence of Different Metal Ions. We next compared k_{pol} and $K_{d,app}$ of WT Pol β toward dATPαS diastereomers in the presence of different metal ions. The ratio $k_{pol}/K_{d,app}$ denotes the substrate specificity of the enzyme. The data are summarized in Table 2 and indicate that the k_{pol} values for dATPαS isomers are lower than the corresponding values for dATP by factors of 2−50. However, the $K_{d,app}$ values are also significantly lower for dATPαS,

Table 1: Pre-Steady-State Kinetic Parameters of WT Pol β and Mutant D27R with dATP Substrates in the Presence of Different Metal Ions

enzyme	metal ion	k_{pol} (s^{-1})	$K_{d,app}$ (μM)	$k_{pol}/K_{d,app}$ (M^{-1} s^{-1})
WT[a]	Mg^{2+}	26.4 ± 0.9	32.2 ± 4.1	820000
WT[a]	Mn^{2+}	19.2 ± 0.7	27.9 ± 2.6	688000
WT[b]	Cd^{2+}	0.065 ± 0.0046	2.6 ± 0.90	25000
D276R	Mg^{2+}	8.6 ± 0.87	13 ± 4.3	660000
D276R	Mn^{2+}	2.3 ± 0.10	3.6 ± 0.58	640000
D276R	Cd^{2+}	ND[c]	ND	ND

[a] These data differ slightly from those published previously (*5*, *25*) due to the different conditions used in this study. [b] All reactions with Cd^{2+} as divalent metal cation were performed in 50 mM Hepes buffer at pH 8.0. All other reactions with Mg^{2+} or Mn^{2+} were performed in 50 mM Tris buffer at pH 8.0. [c] There was no detectable turnover for D276R mutant with Cd^{2+} as the divalent cation.

Table 2: Pre-Steady-State Kinetic Parameters of WT Pol β and Mutant D276R with dATPαS Diastereomers in the Presence of Different Metal Ions

enzyme	metal ion	stereo-isomer	k_{pol} (s^{-1})	$K_{d,app}$ (μM)	$k_{pol}/K_{d,app}$ (M^{-1} s^{-1})
WT	Mg^{2+}	Sp	5.32 ± 0.20	3.3 ± 0.4	1610000
WT	Mg^{2+}	Rp	0.63 ± 0.033	22.3 ± 3.1	28000
WT	Mn^{2+}	Sp	0.69 ± 0.025	1.1 ± 0.23	630000
WT	Mn^{2+}	Rp	0.38 ± 0.038	4.6 ± 1.3	83000
WT	Cd^{2+}	Sp	0.047 ± 0.0012	1.2 ± 0.13	39000
WT	Cd^{2+}	Rp	0.010 ± 0.002	5.6 ± 1.8	1800
D276R	Mg^{2+}	Sp	0.95 ± 0.09	5.0 ± 0.79	190000
D276R	Mg^{2+}	Rp	0.3 ± 0.033	2.4 ± 0.19	130000
D276R	Mn^{2+}	Sp	0.16 ± 0.0027	0.71 ± 0.075	220000
D276R	Mn^{2+}	Rp	0.13 ± 0.005	2.2 ± 0.41	59000
D276R	Cd^{2+}	Sp	0.0034 ± 0.00053	23 ± 9.6	150
D276R	Cd^{2+}	Rp	0.0011 ± 0.00072	10.6 ± 0.25	100

Table 3: Substrate Stereoselectivity of WT Pol β and Mutant D276R toward dATPαS Diastereomers

enzyme	metal ion	(Sp/Rp)k_{pol}	(Sp/Rp)$K_{d,app}$	$(k_{pol}/K_{d,app})_{Sp}/(k_{pol}/K_{d,app})_{Rp}$
WT	Mg^{2+}	8.4	0.15	57.5
WT	Mn^{2+}	1.8	0.24	7.6
WT	Cd^{2+}	4.7	0.21	21
D276R	Mg^{2+}	3.2	2.1	1.5
D276R	Mn^{2+}	1.2	0.32	3.7
D276R	Cd^{2+}	3.1	2.2	1.5

with the exception of the Rp isomer in the presence of Cd^{2+}. As a result, Sp-dATPαS is a slightly better substrate (higher $k_{pol}/K_{d,app}$ ratio) than dATP for WT Pol β in the presence of Mg^{2+}.

The stereoselectivity, defined as $(k_{pol}/K_{d,app})_{Sp}/(k_{pol}/K_{d,app})_{Rp}$ (abbreviated the Sp/Rp ratio), is shown in Table 3. Overall, WT Pol β accepts both isomers but with a preference toward the Sp isomer. The Rp isomer displays lower k_{pol} and higher K_d values for all three metal ions. The Sp/Rp ratios are 57.5, 7.6, and 21, respectively, in the presence of Mg^{2+}, Mn^{2+}, and Cd^{2+}. These data indicate that, although substitution of Mg^{2+} by the "softer" metal ions (which prefer sulfur ligands over oxygen ligands in the order $Mg^{2+} < Mn^{2+} < Cd^{2+}$) (*29*) caused some relaxation of stereoselectivity, it did not follow the expected order and did not lead to a reversal of stereoselectivity.

Pre-Steady-State Kinetic Analyses of D276R Mutant in the Presence of Different Metal Ions. The stereoselectivity of Pol β toward dNTPαS isomers should be dictated mostly by the interactions between the α-phosphate of dNTP and enzymatic residues or metal ions. The crystal structures of ternary complexes of Pol β show no direct interaction between the enzyme and the nonbridging oxygens of the α-phosphate of dNTP (*11*, *13*). On the basis of the crystal structure and protein modeling, we predict that replacing Asp276 with Arg will likely introduce a new hydrogen bonding between the enzyme and the pro-Sp oxygen of the α-phosphate of dNTP and that such a new interaction will likely perturb the stereoselectivity of Pol β.

The D276R mutant was then constructed to test whether the stereoselectivity of Pol β toward dATPαS isomers can be changed. First, we measured the catalytic activity and dissociation constant of regular nucleotide dATP for this mutant protein in the presence of different metal ions. As shown in Table 1, D276R displays a small decrease (by a factor of 3) in k_{pol} relative to WT Pol β with Mg^{2+} as the divalent ion and a moderate decrease (by a factor of 8) with Mn^{2+}. There was no detectable activity for D276R mutant with Cd^{2+} as the divalent metal ion in the reaction. The $K_{d,app}$ of dATP of this mutant is also lower than that of WT Pol β, suggesting a tighter binding of nucleotide for the D276R mutant. This supports enhanced interaction between the enzyme and the nucleotide. As a consequence of decreases in both k_{pol} and $K_{d,app}$, the substrate specificity $k_{pol}/K_{d,app}$ toward dATP is comparable between D276R and WT in the presence of Mg^{2+} or Mn^{2+}.

Stereoselectivity of D276R Pol β toward Stereoisomers of dATPαS in the Presence of Different Metal Ions. We then examined the stereoselectivity of the D276R mutant toward dATPαS diastereomers with different metal ions, and the results are summarized in the lower half of Table 2 (k_{pol} and $K_{d,app}$ values) and Table 3 (Sp/Rp ratios). As shown by the data, the Sp/Rp ratio decreases from 57.5 for WT to 1.5 for D276R in the presence of Mg^{2+}. This result confirms our prediction that the newly introduced positive side chain may interact with the pro-Sp oxygen of α-phosphate and relax the stereoselectivity of Pol β. Most importantly, whereas Sp-dATPαS is a worse substrate for D276R ($k_{pol}/K_{d,app} = 1.9 \times 10^5$ M^{-1} s^{-1}) than for WT ($k_{pol}/K_{d,app} = 1.61 \times 10^6$ M^{-1} s^{-1}), the Rp isomer is a substantially better substrate for D276R ($k_{pol}/K_{d,app} = 1.3 \times 10^5$ M^{-1} s^{-1}) than for WT ($k_{pol}/K_{d,app} = 2.8 \times 10^4$ M^{-1} s^{-1}). The enhancement in the reactivity of the Rp isomer is mainly due to enhanced binding—a decrease in K_d by a factor of 10. As shown in Table 3, the stereoselectivities of the D276R mutant in the presence of Mn^{2+} and Cd^{2+} are also close to 1.

DISCUSSION

This work represents the first use of pre-steady-state kinetics to study the metal ion dependence and dNTPαS stereoselectivity for a DNA polymerase, as well as the first example of altering the Sp- vs Rp-dNTPαS stereoselectivity via site-directed mutagenesis. The potential significance of this work is elaborated below.

Comparison of dATPαS Stereoselectivity between Pol β and Pol I. Although the results of pre-steady-state kinetics cannot be compared directly with those of steady-state kinetic analyses, it is useful to compare the stereoselectivity of Pol β from this work with that of Pol I in a previous work (*22*). In both studies, the enzyme was shown to prefer the Sp

isomer of dATPαS in the presence of Mg^{2+}. However, Pol I showed <0.2% activity toward the Rp isomer, whereas Pol β incorporates the Rp isomer at ~2% activity relative to the Sp isomer. Because replacing Mg^{2+} with the more thiophilic metal ion Co^{2+}, Mn^{2+}, or Zn^{2+} did not increase the activity of the Rp isomer, the authors concluded that the α-phosphate of dNTP is not chelated by a divalent metal ion in Pol I. Instead, they suggested that the negative charge of the α-phosphate is probably neutralized by a positively charged group from the enzyme. For Pol β, replacing Mg^{2+} with Mn^{2+} caused a significant relaxation in stereoselectivity (the Sp/Rp ratio decreased from 57.5 to 7.6). The differences between the results of the two studies could be attributed to differences in the active site structures of the two polymerases or to differences between pre-steady-state and steady-state analyses. However, the results for Pol β are more consistent with subsequent structural studies of DNA polymerases as explained in the next two paragraphs.

(a) As pointed out by Pelletier et al., the interpretation of the results of Pol I was in contradiction with the observation that when dATPαS was cocrystallized with Pol β in the presence of Mn^{2+}, the Rp isomer instead of the Sp isomer binds to the active site (*24*). Our results, however, are more in line with the crystallographic results. In the presence of Mn^{2+} both Sp and Rp diastereomers of dATPαS can be incorporated by WT Pol β. Although Sp is the preferred substrate over Rp, the stereoselectivity is relatively modest (Sp/Rp = 7.6), and $K_{d,app}$ is higher by a modest 4-fold for the Rp isomer. Such a difference is very small in terms of binding energy, and it is not unreasonable that the enzyme cocrystallizes with the slightly less favored Rp isomer.

(b) The structures of *E. coli* Klenow fragment (*30*) and other members of the DNA polymerase I or A family, such as a *Bacillus* DNA polymerase I (*31*), *Thermus aquaticus* DNA polymerase (*32*), and T7 DNA polymeras (*33*), as well as T7 RNA polymerase (*34*), reveal no positively charged enzymatic groups near the α-phosphate. Instead, there are two Mg^{2+} ions neutralizing the charge on α-phosphate as shown in Figure 1: the nucleotide-binding ion A contacts nonbridging oxygens of all three phosphates of the incoming nucleotide, including the pro-Rp oxygens of the α- and β-phosphate. The catalytic metal ion B contacts the pro-Rp oxygen of the α-phosphate of dNTP. Although replacing Mg^{2+} with Cd^{2+} was unable to reverse the stereoselectivity of Pol β toward isomers of dATPαS, the notable relaxation caused by Mn^{2+} is consistent with the coordination of metal ion to the α-phosphate of dNTP. In Pol β, a third aspartic acid (Asp256) interacts with metal ion B, whereas in Pol I a water molecule serves as the ligand at this position. Such subtle structural differences in the active site of enzymes could influence the stereoselectivity in the presence of different metal ions.

Metal Ion Binding Modes of DNA Polymerase β. The first observation of a polymerase complex with both primer-template DNA and dNTP·Mg bound that directly showed the structural basis of a two-metal-ion mechanism was a 2.9 Å ternary structure of rat Pol β (*11*). Later, a higher resolution structure (2.1 Å) of human Pol β complexed with a gapped DNA substrate and ddCTP (*13*) showed detailed interactions between two hexacoordinated, partially hydrated Mg^{2+} ions and the triphosphate moiety of dNTP. Our kinetic data agree with the structures, which predict that Pol β should be

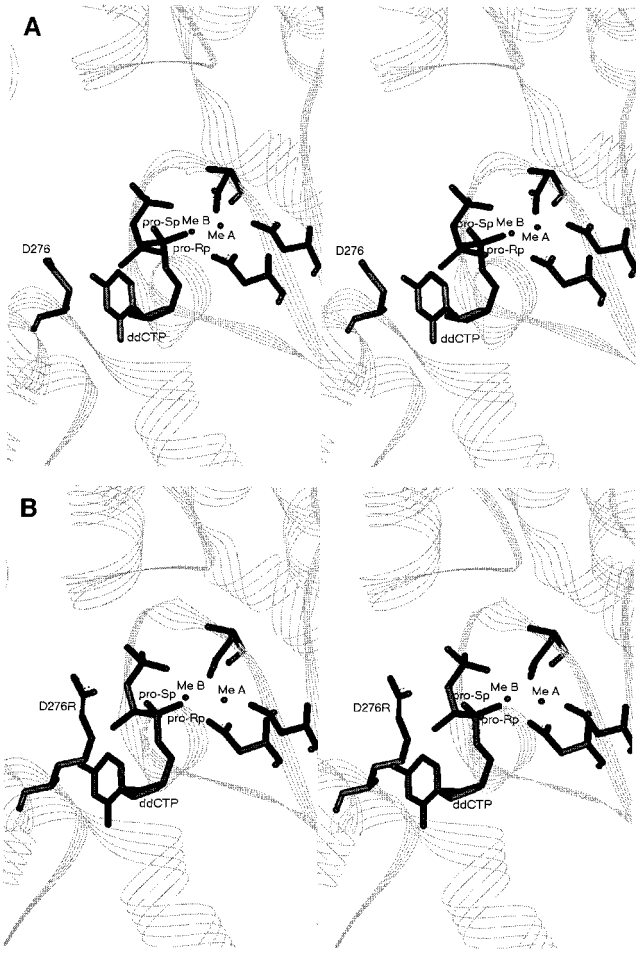

FIGURE 6: Stereoviews of the interactions between Asp276 (A) and the mutated residue Arg276 (B) with the incoming dNTP in the ternary complex. Both were adapted from PDB file 1BPY (*13*) and prepared with WebLabview. Swiss-PdbViewer (*38*) was used to construct the model structure for D276R mutant complexed with DNA substrate and ddNTP shown in (B). The model has been energy minimized. The distance between the Arg side chain and the pro-Sp oxygen of α-phosphate is ~3.7 Å, which is ~3 Å shorter than that with the pro-Rp oxygen.

selective for the Sp isomer of dATPαS when Mg^{2+} is the metal ion in the reaction mixture. Mg^{2+} coordinates oxygen much more strongly than sulfur, and in the active site (Figure 1) both Mg^{2+} ions in the metal sites B and A coordinate the pro-Rp oxygen of the α-phosphate of the nucleotide. If the pro-Rp oxygen is replaced by a sulfur, which is the case for the Rp isomer, coordination by the Mg^{2+} ion in sites B and A should be weakened considerably. On the other hand, replacing the pro-Sp oxygen by sulfur should not affect Mg^{2+} binding to the nucleotide. As expected, the activity of Sp-dATPαS is comparable to (or even slightly better than) that of dATP on the basis of $k_{pol}/K_{d,app}$ ratios.

One might ask why the Rp isomer did not become the preferred isomer when Mg^{2+} is replaced by Cd^{2+}. Possible reasons include complications caused by the two metal ions. It is important to recognize that, although reversal of stereoselectivity by replacing Mg^{2+} with Cd^{2+} would be positive evidence for direct coordination between the metal ion and the phosphate group, a lack of reversal is not necessarily evidence against direct coordination.

Introducing a New Interaction with the α-Phosphate of dNTP. As mentioned above, there is no Pol β side chain

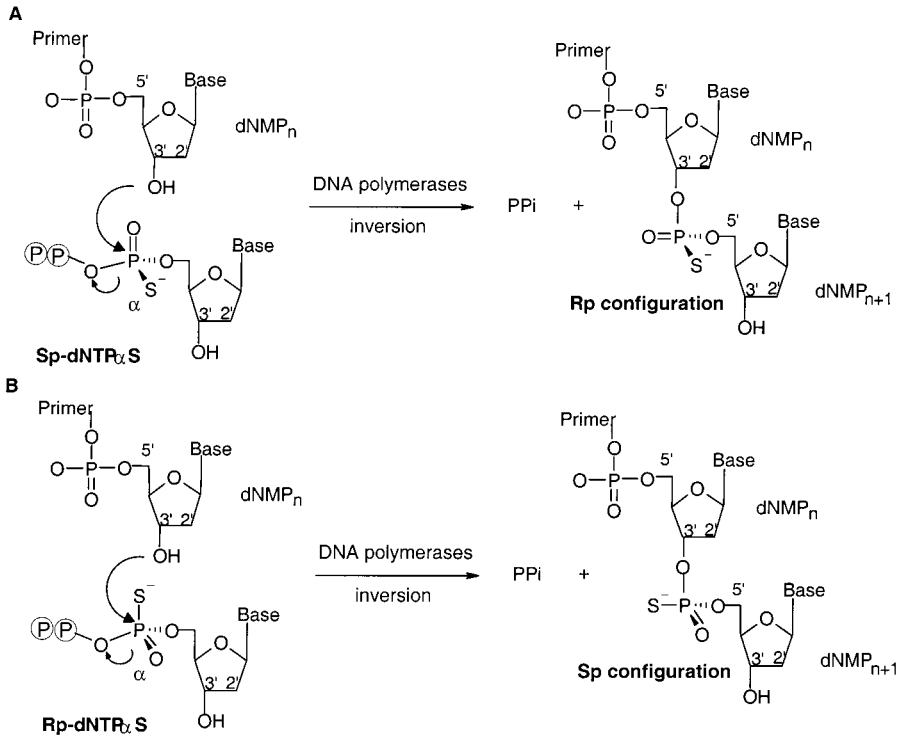

FIGURE 7: Schemes showing the formation of S-oligos with Rp-linkage (A) and Sp-linkage (B).

interacting with the pro-Sp oxygen of the α-phosphate of the incoming nucleotide. On the basis of the crystal structure of the WT Pol β ternary complex (Figure 6A), the β-methylene group of Asp276 is in proximity to the base of the incoming nucleotide. From sequence alignment it is shown that most other X family polymerases have an arginine or lysine at this position (*35*). In addition, Arg72 of the HIV-1 reverse transcriptase is observed to stack with the incoming nucleotide and form hydrogen bonds with the phosphate, and it is highly conserved among reverse transcriptases and telomerases. Mutations of the Arg72 of HIV-RT dramatically lowers the catalytic efficiency of the enzyme (*36*, *37*). On the basis of such information, we constructed the D276R mutant in an attempt to introduce an interaction between the guanidino moiety of arginine and the pro-Sp oxygen of the α-phosphate of dNTP. As shown in the modeled structure generated by the Swiss-PdbViewer (*38*) (Figure 6B), the distance between the pro-Sp oxygen of α-phosphate and the Arg side chain is ~3.7 Å, which is slightly larger than the usual H-bonding distances but is within the range considering this is a modeled structure. Such an interaction is likely to change the stereoselectivity of Pol β toward dNTPαS isomers. A similar approach has been applied to adenylate kinase: it was shown that the stereoselectivity for the conversion of AMPS to (Rp)- or (Sp)-ADPαS can be manipulated by site-directed mutagenesis (*39*, *40*). The Sp/Rp ratio for WT is 95:5, which is completely reversed by the R44M mutation and enhanced to 99.5:0.5 by the R97M mutation. It was noted that, from the crystal structure, both positively charged arginine side chains could interact with the negatively charged phosphoryl group of AMP, but from opposite directions. These interactions were presumably perturbed in the mutants, resulting in perturbed stereoselectivity.

The results suggest that the D276R mutant behaves as predicted. The decrease in the $K_{d,app}$ values indicates a tighter binding between the mutant protein and the incoming nucleotide relative to WT Pol β. In a recently published paper, the D276V mutant was also shown to increase the binding affinity for the incoming nucleotide (*41*). Our results further showed that, in the presence of Mg^{2+}, the stereoselectivity (Sp/Rp ratio) is relaxed by ~40-fold, from 57.5 for WT to 1.5 for D276R. Such a change in the stereoselctivity toward dATPαS is strong evidence that the side chain of Arg276 interacts with the phosphate moiety of the incoming nucleotide.

Enhancement of the Reactivity toward the Rp Isomer by a Single Mutation of Pol β. Although we have not been able to reverse the stereoselectivity of Pol β toward dATPαS isomers either by various metal ions or by site-directed mutagenesis (or the combination of both approaches), we have enhanced the reactivity of the Rp isomer by making a single mutation of the enzyme: the D276R mutant shows a $k_{pol}/K_{d,app}$ ratio of 130000 M^{-1} s^{-1} toward Rp-dATPαS, which is 5 times greater than that of WT (28000 M^{-1} s^{-1}, Table 2). We believe that this represents a significant step in engineering a polymerase capable of specifically incorporating Rp isomers into a DNA oligomer to form S-oligos.

S-oligos are potential antisense drugs as reviewed by Stein (*42*−*44*). Because they are less susceptible to nuclease hydrolysis than regular oligonucleotides, they can form stable duplexes with natural RNA or DNA and stimulate endogenous cellular ribonuclease H activity, which allows for the specific degradation of the target RNA in hybrid duplex. The utility of these derivatives has been recently demonstrated in the many potential antisense applications reported for deoxyoligonucleotides containing such modifications (*45*−*47*). It has been shown that nucleases display a stereoselectivity toward the Rp isomer of S-oligos (*48*), which is generated by incorporating Sp-dNTPαS with inversion of configuration (*49*) at phosphorus as shown in Figure 7. Thus, S-oligos with Sp-linkage (from incorporation of Rp-dNTPαS)

are the preferred isomer for antisense drugs due to their resistance to nucleases. DNA polymerases are specific to the Sp isomer, so only the S-oligos with Rp-linkage can be obtained from enzymatic synthesis. S-oligos with Rp configuration can only be chemically synthesized and then separated from the other isomer. For an oligonucleotide with *n* singly modified internucleotide linkages, there will be 2^n stereomers that make separation complicated. Although ideally a mutant with an even stronger preference toward the Rp isomer of dNTPαS is desirable, the D276R mutant of Pol β has achieved reasonably good activity toward the Rp isomer and represents a significant step toward this goal.

"Thio Effect" of DNA Polymerases. The thio effect, defined as $k_{pol(dATP)}/k_{pol(dATP\alpha S)}$, has been reported for Pol β previously; the small magnitude of the thio effect for correct base pairing (4.3 for T:A) and increased value for incorrect base pairs (e.g., 9 for T:G) have been used as evidence to suggest that the chemical step is not rate-limiting in the catalysis by Pol β (*25*). Similar studies have been reported for Klenow fragment (*50*), T7 polymerase (*51*), and T4 polymerase (*52*). However, recent structural and stopped-flow fluorescence studies have led us to conclude that the chemical step is likely to be the rate-limiting step (or at least partially rate-limiting) in the catalysis reaction of Pol β (*1*). By analyzing the data reported in this paper as described below, we suggest that great caution is needed in using the thio effect as a mechanistic probe.

The ratio $k_{pol(dATP)}/k_{pol(dATP\alpha S)}$ reported in this paper is 26.4/5.3 = 5.0 for dATP/Sp-dATPαS in the presence of Mg^{2+}, which is similar to the thio effect reported previously (*25*). However, the previous studies used a mixture of isomers (Rp + Sp). If pure Rp isomer is used (also in the presence of Mg^{2+}), the thio effect should be 26.4/0.63 = 42. The large difference between the two isomers should reflect the difference in the "intrinsic thio effect" (defined as the observed thio effect when the chemical step is fully rate-limiting), which appears to be very sensitive to the configuration at phosphorus. It is possible that the intrinsic thio effect of incorrect nucleotides is different from that of correct nucleotides, due to changes in the geometry of the phosphorothioate group at the transition state. Thus, in the absence of knowledge about the intrinsic thio effect for each substrate, one cannot conclude whether the chemical step is rate-limiting on the basis of the observed thio effect.

ACKNOWLEDGMENT

We thank Dr. Ru-Tai Jiang for technical assistance in preparing the diastereomers of dATPαS and Xuejun Zhong and Alexander K. Showalter for helpful discussions.

REFERENCES

1. Arndt, J. W., Gong, W., Zhong, X., Showalter, A. K., Liu, J., Donlup, C. A., Chan, M. K., and Tsai, M. D. (2001) *Biochemistry 40*, 5368−5375.
2. Singhal, R. K., Prasad, R., and Wilson, S. H. (1995) *J. Biol. Chem. 270*, 949−957.
3. Sobol, R. W., Horton, J. K., Kuhn, R., Gu, H., Singhal, R. K., Prasad, R., Rajewsky, K., and Wilson, S. H. (1996) *Nature 379*, 183−186.
4. Nicholl, I. D., Nealon, K., and Kenny, M. K. (1997) *Biochemistry 36*, 7557−7566.
5. Ahn, J., Werneburg, B. G., and Tsai, M. D. (1997) *Biochemistry 36*, 1100−1107.
6. Ahn, J., Kraynov, V. S., Zhong, X., Werneburg, B. G., and Tsai, M. D. (1998) *Biochem J. 331*, 79−87.
7. Kraynov, V. S., Werneburg, B. G., Zhong, X., Lee, H., Ahn, J., and Tsai, M. D. (1997) *Biochem J. 323*, 103−111.
8. Kraynov, V. S., Showalter, A. K., Liu, J., Zhong, X., and Tsai, M. D. (2000) *Biochemistry 39*, 16008−16015.
9. Osheroff, W. P., Beard, W. A., Wilson, S. H., and Kunkel, T. A. (1999) *J. Biol. Chem. 274*, 20749−20752.
10. Shah, A. M., Li, S.-X., Anderson, K. S., and Sweasy, J. B. (2001) *J. Biol. Chem.* (in press).
11. Pelletier, H., Sawaya, M. R., Kumar, A., Wilson, S. H., and Kraut, J. (1994) *Science 264*, 1891−1903.
12. Pelletier, H., Sawaya, M. R., Wolfle, W., Wilson, S. H., and Kraut, J. (1996) *Biochemistry 35*, 12742−12761.
13. Sawaya, M. R., Prasad, R., Wilson, S. H., Kraut, J., and Pelletier, H. (1997) *Biochemistry 36*, 11205−11215.
14. Steitz, T. A., Smerdon, S. J., Jager, J., and Joyce, C. M. (1994) *Science 266*, 2022−2025.
15. Bessman, M. J., Lehman, I. R., Simms, E. S., and Kornberg, A. (1958) *J. Biol. Chem. 233*, 171−177.
16. Kornberg, A., and Baker, T. A. (1992) *DNA Replication*, 2nd ed., Freeman, San Francisco, CA.
17. Burgers, P. M. J., Sathyanarayana, B. K., Saenger, W., and Eckstein, F. (1979) *Eur. J. Biochem. 100*, 585−691.
18. Burgers, P. M. J., and Eckstein, F. (1980) *J. Biol. Chem. 255*, 8229−8233.
19. Armstrong, V. W., Yee, D., and Eckstein, F. (1979) *Biochemistry 18*, 4120−4123.
20. Jaffe, E. K., and Cohn, M. (1979) *J. Biol. Chem. 254*, 10839−10845.
21. Eckstein, F. (1983) *Angew. Chem. 95*, 431−447.
22. Burgers, P. M., and Eckstein, F. (1979) *J. Biol. Chem. 254*, 6889−6893.
23. Romaniuk, P. J., and Eckstein, F. (1982) *J. Biol. Chem. 257*, 7684−7688.
24. Pelletier, H., Sawaya, M. R., Wolfle, W., Wilson, S. H., and Kraut, J. (1996) *Biochemistry 35*, 12762−12777.
25. Werneburg, B. G., Ahn, J., Zhong, X., Hondal, R. J., Kraynov, V. S., and Tsai, M. D. (1996) *Biochemistry 35*, 7041−7050.
26. Casas-Finet, J. R., Kumar, A., Morris, G., Wilson, S. H., and Karpel, R. L. (1991) *J. Biol. Chem. 266*, 19618−19625.
27. Eckstein, F., and Goody, R. S. (1976) *Biochemistry 15*, 1685−1691.
28. Brody, R. S., and Frey, P. A. (1981) *Biochemistry 20*, 1245−1252.
29. Jaffe, E. K., and Cohn, M. (1978) *J. Biol. Chem. 253*, 4823−4825.
30. Beese, L. S., Friedman, J. M., and Steitz, T. A. (1993) *Biochemistry 32*, 14095−14101.
31. Kiefer, J. R., Mao, C., Braman, J. C., and Beese, L. S. (1998) *Nature 391*, 304−307.
32. Kim, Y., Eom, S. H., Wang, J., Lee, D.-S., Suh, S. W., and Steitz, T. A. (1995) *Nature 376*, 612−616.
33. Doublie, S., Tabor, S., Long, A. M., Richardson, C. C., and Ellenberger, T. (1998) *Nature 391*, 251−258.
34. Jeruzalmi, D., and Steitz, T. A. (1998) *EMBO J. 17*, 4101−4113.
35. Oliveros, M., Yanez, R. J., Salas, M. L., Salas, J., Vinuela, E., and Blanco, L. (1997) *J. Biol. Chem. 272*, 30899−30910.
36. Sarafianos, S. G., Pandey, V. N., Kaushik, N., and Modak, M. J. (1995) *J. Biol. Chem. 270*, 19729−19735.
37. Lewis, D. A., Bebenek, K., Beard, W. A., Wilson, S. H., and Kunkel, T. A. (1999) *J. Biol. Chem. 274*, 32924−32930.
38. Guex, N., and Peitsch, M. C. (1997) *Electrophoresis 18*, 2714−2723.
39. Dahnke, T., Jiang, R. T., and Tsai, M. D. (1991) *J. Am. Chem. Soc. 113*, 9388−9389.
40. Jiang, R. T., Dahnke, T., and Tsai, M. D. (1991) *J. Am. Chem. Soc. 113*, 5485−5486.
41. Vande Berg, B. J., Beard, W. A., and Wilson, S. H. (2001) *J. Biol. Chem. 276*, 3408−3416.
42. Stein, C. A., Ed. (1998) *Applied Antisense Oligonucleotide Technology*, Wiley-Liss, New York.

43. Stein, C. A. (1996) *Trends Biotechnol. 14*, 147−149.
44. Stein, C. A. (1996) *Chem. Biol. 3*, 319−323.
45. Stein, C. A., and Cohen, J. S. (1988) *Cancer Res. 48*, 2659−2668.
46. Miller, P. S., and Ts'o, P. O. P. (1987) *Anti-Cancer Drug Des. 2*, 117−128.
47. Uhlmann, E., and Peyman, A. (1990) *Chem. Rev. 90*, 543−584.
48. Brautigam, C. A., Sun, S., Piccirilli, J. A., and Steitz, T. A. (1999) *Biochemistry 38*, 696−704.
49. Gupta, A. P., and Benkovic, S. J. (1984) *Biochemistry 23*, 5874−5881.
50. Kuchta, R. D., Mizrahi, V., Benkovic, P. A., Johnson, K. A., and Benkovic, S. J. (1987) *Biochemistry 26*, 8410−8417.
51. Patel, S. S., Wong, I., and Johnson, K. A. (1991) *Biochemistry 30*, 511−525.
52. Capson, T. L., Peliska, J. A., Kaboord, B. F., Frey, M. W., Lively, C., Dahlberg, M., and Benkovic, S. J. (1992) *Biochemistry 31*, 10984−10994.

BI010646J